The S(¹D) + N_2 Quenching Process: Determination of Branching Ratios to Triplet Fine Structure Products

G. C. McBane,† I. Burak,‡ G. E. Hall,§ and P. L. Houston*

Department of Chemistry, Cornell University, Ithaca, New York 14853 *(Received: July 22, 1991; In Final Form: September 17, 1991)*

The quenching by N_2 of S(¹D) to the S($^3P_2$), S($^3P_1$), and S($^3P_0$) levels has been investigated by using tunable vacuum-ultraviolet laser-induced fluorescence to probe the initial and final levels following creation of S(¹D) by pulsed 222-nm photolysis of OCS. The total quenching rate is $(7.1 \pm 1.0) \times 10^{-11}$ cm^3 molecule^{-1} s^{-1}, while the branching ratios were found to be 0.143 ± 0.006 for $^3P_0$, 0.085 ± 0.012 for $^3P_1$, and 0.77 ± 0.02 for $^3P_2$. The total rate is in good agreement with previous measurements. The branching ratios contrast to the inverted distribution found by Stout, Andrews, Bevilacqua, and Weisman for quenching of S(¹D) by argon [*Chem. Phys. Lett.* **1988**, *151*, 156].

I. Introduction

Relaxation processes are generally classified as "spin allowed" or "spin forbidden" depending on whether or not the vector sum of the electron spins of the reactants is equal to that of the products. However, some atom–molecule collision processes violate the spin correlation rules. Relaxation processes of O(¹D) atoms by singlet molecular, species, for example, are characterized by fast rate constants even though the final products, O(^3P) and the singlet molecule, require a change in total spin. Within this class of spin-forbidden systems, the relaxation rate of O(¹D) by molecular nitrogen has received the most extensive study. The fast rate constant reported[1] for this relaxation process has been explained in terms of crossing between the bound singlet and repulsive triplet potential surfaces of the N_2O molecule.[2-4] The involvement of an N_2O collision complex has been suggested by deMore and Raper,[2] Tully,[5] and Zahr et al.[6] as a mechanism for increasing the deactivation probability. While theory and experiment for the total deactivation rate constant are in qualitative agreement, the branching ratio among the fine structure components of the O(^3P) has only recently been determined experimentally[7] and has not been predicted theoretically.

The similar relaxation of S(¹D) atoms by molecular nitrogen has also been studied. Both the total deactivation rate[8,9] and the rate of equilibration among the $^3P_2$, $^3P_1$, and $^3P_0$ states of the sulfur atom have been measured experimentally,[10] but the branching ratios for relaxation into the $^3P_2$, $^3P_1$, and $^3P_0$ fine structure components of the sulfur atom have not been determined, nor has any theoretical work been reported on this system. This article reports an examination of the S(¹D) quenching by nitrogen and determines the branching ratios for the first time.

II. Experimental Section

Apparatus. Pulsed photolysis of OCS at 222 nm was used to create S(¹D) atoms in a cell containing large excesses of N_2 and He. Nearly all the atomic sulfur is produced in the ¹D state.[11] The population of each of the S($^3P_{0,1,2}$) levels was then monitored as a function of time using laser-induced fluorescence (LIF). The nitrogen served both to quench the excited sulfur atoms and to relax the different triplet levels among themselves. The helium helped to prevent diffusion of the sulfur species out of the detection zone and also contributed to the relaxation of the fine structure levels.

The experiments were performed in a glass cell fitted with entrance and exit windows for the 222-nm dissociation beam and the vacuum-ultraviolet (vacuum-UV) probe beam and an exit window for the fluorescence, as shown in Figure 1. In order to both minimize absorption of the vacuum-UV fluorescence by OCS and provide sufficient volume to avoid problems of photoproduct buildup, the cell had the shape of a cylinder with the fluorescence window at the top and the arms for the laser beams just underneath it.

TABLE I: Transitions and Probe Frequencies Used To Monitor Sulfur Populations

state	transition	energy, cm^{-1}
$^1D_2$	$^1P_1 \leftarrow {}^1D_2$	69 051
$^3P_2$	$^3D_3 \leftarrow {}^3P_2$	67 843
$^3P_1$	$^3D_2 \leftarrow {}^3P_1$	67 429
$^3P_0$	$^3D_1 \leftarrow {}^3P_0$	67 243

A Quanta-Ray laser system (DCR-2A, PDL-2, WEX) provided roughly 2 mJ/pulse of 222-nm light at 10 Hz. The beam was loosely focused to a diameter of 2–3 mm inside the cell. After passing through the gas cell, the transmitted light struck a quartz cuvette filled with Rhodamine dye. Fluorescence from the cuvette was monitored with a photodiode and used to normalize the LIF signals for fluctuations in the power of the photolysis laser.

The vacuum-UV probe light for LIF detection of S(^3P) was generated by four-wave mixing in magnesium vapor. Details of the apparatus may be found elsewhere.[11] Briefly, the beams from two pulsed dye lasers (Lambda Physik FL2000E) pumped by a dual-cavity XeCl laser (Lambda EMG150ES) were combined by four-wave mixing in magnesium vapor to produce the output frequency $2\omega_1 + \omega_2$. Table I shows the transitions and frequencies used to probe the ^3P sulfur states. To provide the appropriate wavelengths, Coumarin 440 dye was used for ω_1 and Coumarin 480 was used for ω_2. The transmitted vacuum-UV power was measured with a solar-blind photomultiplier whose output was used to normalize the LIF signals.

Timing between the two laser pulses was accomplished by using the gate delay of a boxcar integrator as a scanning delay generator. The delay between the photolysis and probe lasers was scanned from 0 to 8.5 μs. The LIF signal for a particular triplet component was detected with an $f/1$ imaging system and a solar-blind photomultiplier (EMR 542G–09–17). The signals were averaged in

† Current address: Chemical Dynamics Laboratory, Department of Chemistry, University of Minnesota, Minneapolis, MN 55455.
‡ Permanent address: Department of Chemistry, University of Tel Aviv, Tel Aviv, Israel.
§ Current address: Chemistry Department, Brookhaven National Laboratory, Upson, NY 11973.
* To whom correspondence should be addressed.

(1) Heidner, R. F.; Husain, D.; Wiesenfeld, J. R. *J. Chem. Soc., Faraday Trans. 2* **1973**, *69*, 927.
(2) deMore, W.; Raper, O. F. *J. Chem. Phys.* **1962**, *37*, 2048. deMore, W. B.; Raper, D. F. *Astrophys. J.* **1964**, *139*, 1381.
(3) Fisher, E. R.; Bauer, E. *J. Chem. Phys.* **1972**, *57*, 1966.
(4) Delos, B. *J. Chem. Phys.* **1973**, *59*, 2365.
(5) Tully, J. C. *J. Chem. Phys.* **1974**, *61*, 61.
(6) Zahr, G. E.; Preston, R. K.; Miller, W. H. *J. Chem. Phys.* **1975**, *62*, 1127.
(7) Shafer, N.; Tonokura, K.; Matsumi, Y.; Tasaki, S.; Kawasaki, M. *J. Chem. Phys.*, in press.
(8) Black, G.; Jusinski, L. E. *J. Chem. Phys.* **1985**, *82*, 789.
(9) Black, G.; Jusinski, L. E.; Taherian, M. R. *Chem. Phys. Lett.* **1985**, *122*, 93.
(10) Black, G. *J. Chem. Phys.* **1986**, *84*, 1345.
(11) Sivakumar, N.; Hall, G. E.; Houston, P. L.; Burak, I.; Hepburn, J. W. *J. Chem. Phys.* **1988**, *88*, 3692–3708.

0022-3654/92/2096-753$03.00/0

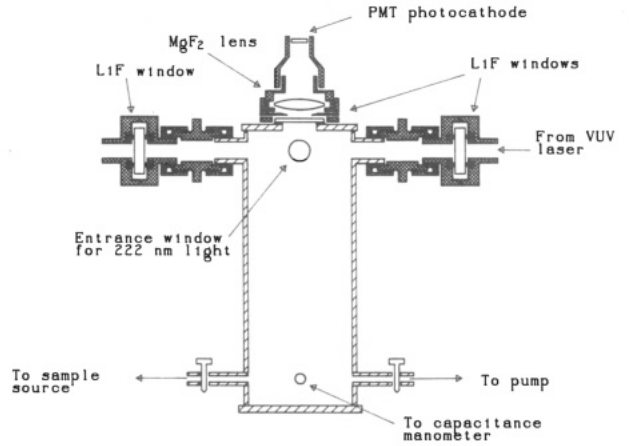

Figure 1. Cell used for kinetics experiments. The vacuum-UV probe beam entered through the LiF windows shown; the 222-nm photolysis beam entered through the quartz window, traveling perpendicular to the plane of the page.

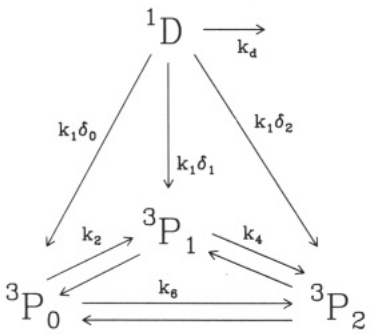

Figure 2. Kinetic scheme for the quenching of $S(^1D)$ and the subsequent relaxation of the ^3P levels. k_d is the diffusional loss of ^1D, and the δ_n are the branching fractions for quenching into the triplet components.

a boxcar integrator (Stanford SRS-250) and collected by an LSI-11 computer.

The OCS used (Matheson) was subjected to several freeze–pump–thaw cycles to remove impurity CO and then distilled from a methanol/liquid nitrogen slush to remove CS_2 and other less volatile impurities. Samples were prepared by successive dilution with nitrogen (Matheson, 99.9995% stated purity) and helium (Spectra-Gases, 99.999%). A capacitance manometer (MKS Baratron) was used to measure the pressures. Experiments of about 5 min in duration were performed on static samples, and the samples were replaced after each scan. The effects of photoproduct buildup were determined to be inconsequential.

Analysis. A complete analysis of the data would require at least 10 rate constants: quenching rate constants into each of the three triplet components, three rate constants for interconversion among triplet states for each of nitrogen and helium, and a diffusion rate, which should be roughly constant for constant total pressure. During the analysis it became clear that the data did not contain enough information to determine all the interconversion rates uniquely. The approximation was then made that the interconversion rate constants for nitrogen should be related to those for helium by a simple multiplicative constant. The analysis, then, determined eight parameters from the data: quenching rates (by N_2) into each of the triplet components, interconversion rates $^3P_0 \rightarrow {}^3P_1$, $^3P_1 \rightarrow {}^3P_2$, and $^3P_0 \rightarrow {}^3P_2$ for helium, an interconversion efficiency ratio for nitrogen relative to helium, and a diffusion rate constant. The kinetic scheme, with the exception of the nitrogen/helium ratio, is thus shown in Figure 2. No evidence of diffusion loss of triplet sulfur was observed, so the diffusion constant was applied only to the singlet state. Note that the reverse rate constants for the interconversion are related to the forward ones through the known equilibrium constants. The quenching of $S(^1D)$ by He has been determined[8] to be more than 3 orders of magnitude slower than quenching by N_2, so it was ignored in this analysis. Absolute amplitudes for the triplet components were not used in the fit because they may be affected by such factors as slight changes in the vacuum-UV wavelength between scans and variations in the OCS absorption of the fluorescence with fluorescence wavelength. We report below the total quenching constant and branching ratios into the individual triplet components.

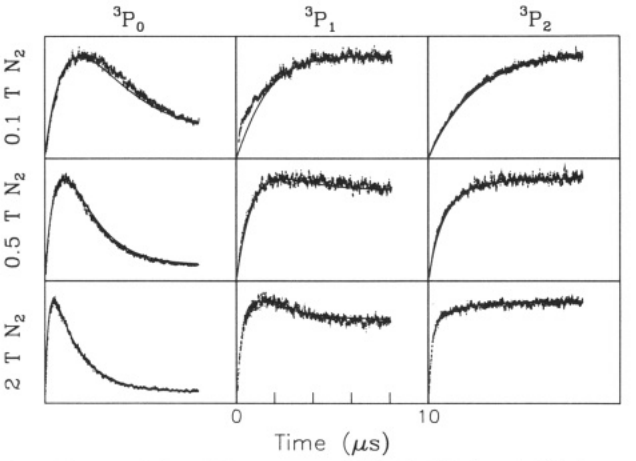

Figure 3. Laser-induced fluorescence of $S(^3P_0)$, $S(^3P_1)$, and $S(^3P_2)$ as a function of time after the 222-nm photolysis pulse for three different N_2 pressures. The smooth lines through the curves are the best fit using the kinetic parameters reported in the text. All the scans have been scaled to give an arbitrary maximum amplitude of unity. Absolute signals are about the same for the $^3P_0$ and $^3P_1$ traces, while that for $^3P_2$ trace is about 10 times larger.

For the iterative fitting of the prediction of the kinetic scheme to the data, integration by a Runge–Kutta fourth-order method was used to calculate the time evolution of each triplet component given a set of trial rate constants. Powell's method[12] was used to adjust the rate constants in order to minimize the merit function

$$\chi^2 = \sum_{i=1}^{n} \left(\frac{y(i) - y_{\mathrm{calc}}(i)}{\sigma(i)} \right)^2 \qquad (1)$$

where the sum is taken over three data curves at each of three pressures. In order to reduce the computation time and effects of high-frequency noise on the results, the data were smoothed with a sliding-median technique,[12] and the χ^2 sum was then taken over approximately every 20th point. σ_i was taken to be the larger of y_i itself and a small "baseline noise" level at each point. The early parts of the traces, where quenching is important and where the concentrations are changing the fastest, were weighted about twice as heavily as later parts. Further details of the fitting procedure have been provided elsewhere.[13]

III. Results

Figure 3 displays the time-dependent laser-induced fluorescence data for the three different $S(^3P)$ levels at three different total pressures. The three samples each had a total pressure of 5 Torr and an OCS partial pressure of 1 mTorr, but the partial pressure of N_2 was either 100, 500, or 2000 mTorr. Also shown as smooth lines in the figure are the fits to the data using the method described above. The fitting procedure was performed about 20 times with differing initial conditions and weighting systems. The N_2 total quenching rate and the values of the branching ratios were found to be quite independent of initial parameters and fitting characteristics. The total quenching rate obtained was $(7.1 \pm 1.0) \times 10^{-11}$ cm^3 molecule^{-1} s^{-1}, while the branching ratios were found to be $\delta_0 = 0.143 \pm 0.006$ for $^3P_0$, $\delta_1 = 0.085 \pm 0.012$ for $^3P_1$, and $\delta_2 = 0.77 \pm 0.02$ for $^3P_2$. The quoted uncertainties are 95% confidence intervals obtained from many runs of the fitting procedure with different weighting schemes and initial conditions.

(12) Press, W. H.; Flannery, B. P.; Teukoslky, S. A.; Vetterling, W. T. *Numerical Recipes in C: The Art of Scientific Computing*; Cambridge University Press: Cambridge, England, 1988.

(13) McBane, G. C. Ph.D. Thesis, Cornell University, 1990.

We estimate that remaining errors resulting from processes ignored in the kinetic model, primarily quenching by OCS and kinetic energy dependent quenching of the initially fast singlet, will not contribute more than 1% (absolute) uncertainty to the branching ratios. The total rate of singlet quenching is in good agreement with the value reported by Black and Jusinski[8] of $(8.5 \pm 0.9) \times 10^{-11}$ cm^3 molecule^{-1} s^{-1}.

Since we were unable to determine individual rate constants for the interconversion and were forced to make a rather drastic assumption about the ratio of rate constants for relaxation by He and N_2, we have little confidence in the fitted values for He- or N_2-induced interconversion rates. The rates obtained for removal of $^3P_0$ compared well with previously reported values,[9] but the parameters suffered from correlations which we were unable to remove. More detailed experiments are required to obtain reliable values for the relaxation rate constants.

IV. Discussion

Stout et al. have studied the fine structure selectivity of the quenching of $S(^1D)$ by Ar and have found the branching ratio into $^3P_0$ to be about $\delta_0 = 0.8$.[14] They explained the high selectivity in quenching to the $S(^3P_0)$ level in terms of the locations of curve crossings into the different triplet states calculated by a CI method. The calculation showed a small charge-transfer interaction between Ar and $S(^1D)$ which creates a shallow attractive well at an internuclear distance of 2.9 Å. The molecular potential curve which correlates to $S(^3P_2)$ crosses the singlet curve on its repulsive part, about 560 cm^{-1} above the energy of separated atoms. On the other hand, the calculated potential curve which correlates to $S(^3P_0)$ crosses the singlet curve at a point just inside the bottom of the attractive well, at an energy 240 cm^{-1} below that of separated atoms. Since the curve producing $^3P_0$ can be reached with no barrier, and the curve producing $^3P_2$ can only be reached over a barrier of more than $2kT$, Stout et al. expect a large excess of the quenching products in the higher state.

Such high selectivity has not been found in our measurement of the deactivation of $S(^1D)$ by N_2. A statistical model, based solely on the degeneracies of the final states, predicts branching ratios of $\delta_0 = 0.11$, $\delta_1 = 0.33$, and $\delta_2 = 0.56$. Our observed δ_0 value of 0.143 is somewhat higher than the statistical expectation, but not markedly so. The only clear deviation from a statistical model is that $^3P_1$ with an observed $\delta_1 = 0.085$ gets substantially less population in the quenching process than expected.

A somewhat more complex analysis of the curve crossings in N_2S can be performed by considering the splitting of each of the $2J + 1$ M atomic states in the electric field created by the N_2 molecule and correlating the resulting states with electronic states in the linear N_2S molecule. An examination of the effect of bending the N_2S molecule shows that only two of the states correlating to $^3P_1$ and only two of the states correlating to $^3P_2$ have the correct A′ symmetry to mix with the bound singlet curve. If all crossings were to have the same probability, the branching ratios predicted by this model would be $\delta_0 = 0.2$, $\delta_1 = 0.4$, and $\delta_2 = 0.4$ as compared to the observed ratios of $\delta_0 = 0.143$, $\delta_1 = 0.085$, and $\delta_2 = 0.77$. The $^3P_1$ population expected from this model is again larger than that observed. The observed $^3P_0$ branching ratio is slightly lower than expected, as well.

Since the N_2S potential well is probably quite deep, it is unlikely that an explanation similar to the one proposed for Ar + S collisions can predict the observed branching ratios. All the singlet–triplet crossing "seams" are likely to be at larger N_2–S separation than that at the well minimum, at least for geometries near the linear equilibrium structure of N_2S, so it is hard to imagine how the $J = 1$ surface could be crossed less to often than either of the other two.

Previous studies of similar systems[5,6] have made the assumption that the spin–orbit matrix elements connecting each of the triplet components to the singlet have similar magnitudes; it is possible that the $J = 1$ component here is simply not coupled strongly to the singlet. The coupling strength is probably a strong function of geometry, so an accurate calculation would require an average over collision orientations. We have not performed such a calculation.

V. Conclusion

The branching ratios for the production of $S(^3P_{2,1,0})$ in the deactivation of $S(^1D)$ by N_2 were found to be 0.143 ± 0.006 for $^3P_0$, 0.085 ± 0.012 for $^3P_1$, and 0.77 ± 0.02 for $^3P_2$, while the total deactivation rate of $S(^1D)$ by N_2 was found to have a rate constant of $(7.1 \pm 1.0) \times 10^{-11}$ cm^3 molecule^{-1} s^{-1}, in good agreement with previous work by Black and Jusinski.[8] The observed branching ratios are quite different from those found by Stout et al.,[14] who found an inverted $S(^3P)$ distribution in the deactivation of $S(^1D)$ by Ar. While it is possible that a simple theory can reproduce the observed data, it seems more likely that the N_2 branching ratios reported here will provide an challenge for modern molecular collision theory. The atoms involved are relatively heavy, so that calculation of accurate potential surfaces even for the ground state represents a substantial task. In addition, the surface crossing requires an accurate description of the nonadiabatic collision dynamics.

Acknowledgment. This work was supported by the Air Force Office of Scientific Research under Grant AFOSR-89-0162. We thank Dr. C. E. M. Strauss for help with the initial experiments and Professor J. W. Hepburn for suggesting the cell design. Support for G.E.H. at Brookhaven National Laboratory was provided by USDOE, Office of Basic Energy Sciences.

Registry No. COS, 463-58-1; S, 7704-34-9; N_2, 7727-37-9.

(14) Stout, J. E.; Andrews, B. K.; Bevilacqua, T. J.; Weisman, R. B. *Chem. Phys. Lett.* **1988**, *151*, 156.